Benzhydrylpyridinium Ions: A New Class of Thermometer Ions for the Characterization of Electrospray-Ionization Mass Spectrometers

Rene Rahrt,^{†,§} Thomas Auth,^{†,§} Maria Demireva,^{‡,§} P. B. Armentrout,^{*,‡} and Konrad Koszinow-ski,^{*,†}

[†]Institut für Organische und Biomolekulare Chemie, Universität Göttingen, Tammannstraße 2, 37077 Göttingen, Germany

[‡]Department of Chemistry, University of Utah, 315 S. 1400 E., Salt Lake City, UT 84112, USA

ABSTRACT: Previous attempts to characterize the internal energies of ions produced by electrospray ionization (ESI) have chiefly relied upon benzylpyridinium ions, R-BnPy⁺, as thermometer ions. However, these systems are not well suited for this purpose because of their relatively high dissociation energies. Here, we propose benzhydrylpyridinium ions, R,R'-BhPy⁺, as a new class of thermometer ions. DLPNO-CCSD(T)/CBS//PBEo-D₃BJ calculations for R,R'-BhPy⁺ (R,R' = H,H'; Me,Me'; H,OMe'; Me,OMe'; OMe,OMe'; NPh₂,NPh₂') predict that these ions fragment by the loss of pyridine via loose transition states. The computed threshold energies of these fragmentations, $0.70 \le E_0 \le 1.74$ eV, are significantly lower than those of the dissociation of the benzylpyridinium ions. The theoretical predictions agree well with results from guided ion beam experiments, which find threshold energies of 1.79 ± 0.11 , 1.55 ± 0.13 , and 1.37 ± 0.14 eV for the fragmentation of R,R'-BhPy⁺, R,R' = H,H'; Me,Me'; H,OMe', respectively. The determined thermochemistry for these systems is then used to characterize the internal energies of ions produced by ESI from dichloromethane and methanol solutions under standard conditions. Correlating the measured survival yields of five of the R,R'-BhPy⁺ ions with the computed threshold energies including explicit consideration of their dissociation rates, we derive energy distributions with maxima at $2.06 \pm 0.13/1.88 \pm 0.11$ eV and widths of $0.86 \pm 0.07/0.86 \pm 0.06$ eV (dichloromethane/methanol). These energy distributions are comparable to ion temperatures between $620 \pm 20/590 \pm 20$ and $710 \pm 20/680 \pm 20$ K (dichloromethane/methanol).

The advent of electrospray ionization (ESI) has revolutionized mass spectrometry and analytical chemistry as a whole.¹ Despite its countless applications, the mechanism of the ESI process is still not fully understood because of its complexity.² In particular, it is important to know how much energy is imparted to the analyte ions during the ESI process and their transfer into the vacuum system of the mass spectrometer. If sufficient energy is deposited into labile ions, they will undergo fragmentation and, thus, escape detection. Hence, the problem of the effective energy of the ions produced by ESI is of critical practical importance.

Measuring the internal energies of gaseous ions is not trivial. Several spectroscopic studies have made use of temperature-sensitive dyes to determine the temperature of the ions in the ESI plume.³ Despite its elegance, this type of experiment is not easily implemented and therefore does not lend itself for routine measurements. Moreover, it does not capture the effects of energetic collisions between the analyte ions and residual gas in the region following the ESI plume and during the ion transfer toward the mass analyzer. The most common approach to quantify the internal energies of ions produced by ESI

relies on the use of so-called thermometer ions. Such thermometer ions are ions that fragment in a well-defined manner once their internal energies exceed the threshold energies, E_o , associated with these fragmentations.⁴ The observation of surviving intact precursor ions implies that their internal energy has not reached the threshold energy whereas the formation of fragment ions signifies the opposite. It is common practice to use a set of related thermometer ions with different E_o values and to measure the fraction of surviving precursor ions, the so-called survival yield (SY), eq. (1),

$$SY = \frac{I_{\rm P}}{I_{\rm P} + I_{\rm F}} \tag{1}$$

where I_P is the intensity of the intact precursor ion and I_F that of the fragment ion. ⁵ Correlating the measured survival yields with the known E_o thresholds then results in a sigmoidal plot, whose derivative yields a Gaussian-like function reflecting the internal energy distribution of the ions under the probed experimental conditions. ⁵ In a more sophisticated treatment, the non-instantaneous nature of the decomposition process is taken into account: ions, whose internal energy just exceeds the

threshold, may dissociate too slowly to allow the observation of the fragmentation process within the experimental time window. The extra energy required to accelerate the fragmentation sufficiently such that it becomes observable is commonly referred to as kinetic shift and can be estimated by rate calculations.⁶⁷

The vast majority of thermometer ions used so far for characterizing the energetic conditions of the ESI process correspond to benzylpyridinium ions, R-BnPy⁺.5,8 With the known exceptions of NO₂-BnPy⁺ and I-BnPy⁺,⁹ these ions decompose by the simple loss of pyridine in a single fragmentation channel, which is an important requirement for thermometer ions (Scheme 1, top).10 By changing the substituent in the para position of the benzyl group, the electronic properties of the aromatic ring and, thus, the dissociation energies of the R-BnPy+ ions can be finetuned in a straightforward manner. Moreover, the R-BnPy+ ions are easily synthesized and afford high ESI signal intensities. These advantageous features explain the popularity of these systems as thermometer ions.^{5,8,11-14} However, until very recently, no sufficiently accurate experimental values for the R-BnPy⁺ dissociation energies were available.15 Thus, earlier work applied threshold energies determined by quantum chemical calculations, whose accuracy was only rather limited.^{5,8a-f,11-13} As a consequence, the conclusions drawn from these early studies are doubtful. Later calculations pointed to R-BnPy+ dissociation energies substantially higher than predicted originally. 8g,14,16 This result was fully borne out by experiments performed by Armentrout and co-workers.¹⁷ Threshold collision-induced dissociation (TCID) studies found $E_o(R-BnPy^+) \ge 1.93 \pm 0.08 \text{ eV}$. Furthermore, this study determined kinetic shifts, which were significantly lower than previous estimates. 8c,e,g,h The relatively high Eo values reflect the fact that R-BnPy+ ions are not well suited for characterizing the ESI process under typical conditions (for example, only 10% dissociation of OMe-BnPy+, the most weakly bound system, resulting from in-source fragmentation).17 Indeed, harsher conditions have been deliberately used in the ion transfer to facilitate the fragmentation of R-BnPy+ thermometer ions and observe the effects of different instrumental settings.86 Clearly, thermometer ions with lower threshold energies are needed for characterizing the ESI process accurately.

Scheme 1. Comparison of conventional and new thermometer ions and their fragmentation reactions.

Previous work: benzylpyridinium ions

R-BnPy⁺

• lower stabilities of fragment primary carbocations
• relatively high
$$E_0$$

This work: benzhydrylpyridinium ions

R,R'-BhPy⁺

• higher stabilities of fragment secondary carbocations
• relatively low
$$E_0$$

We sought to develop such new thermometer ions and at the same time to maintain the aforementioned advantages of the R-BnPy⁺ ions. Our idea was to weaken the C-N bond of the R-BnPy+ scaffold and lower its dissociation energy by stabilizing the benzyl fragment ion R-Bn⁺. ^{18,19} To this end, we introduce a second aryl substituent (Scheme 1, bottom). The resulting benzhydrylium ions, R,R'-Bh+, are well-known. Mayr and coworkers have systematically studied their condensed-phase chemistry, including their synthesis, and established them as reference electrophiles for determining the nucleophilicity of a wide range of compound classes.20 Likewise, benzhydrylium ions have been established as valuable reference electrofuges and Lewis acids.20c,e,f These investigations included the reactions of R,R'-Bh+ with pyridine to afford benzhydrylpyridinium ions R,R'-BhPy+ as well as the heterolytic dissociation of the latter.20e,f,21

Here, we explore the suitability of benzhydrylpyridinium ions as thermometer ions for characterizing the ESI process. First, we use high-level quantum chemical methods to calculate their dissociation energies. For selected examples, we check the validity of the obtained values by TCID experiments. Moreover, we calculate the fragmentation rates of the R,R'-BhPy⁺ ions to estimate the kinetic shifts associated with their dissociation under typical conditions. We then apply the new thermometer ions to characterize the effective energies imparted to analyte ions during the ESI process and the subsequent ion transfer into a commercial mass spectrometer.

COMPUTATIONAL AND EXPERIMENTAL SECTION

Quantum Chemical Calculations. If not stated otherwise, Gaussian o9²² was used for geometry optimizations and harmonic vibrational frequency calculations. Additional single point energy (SPE) calculations as well as potential energy surface scans were performed with the software package ORCA 4.0.²³ Molecular structures in-

volved in the dissociations of R,R'-BhPy+ and R-BnPy+ ions were optimized with the dispersion-corrected hybrid functional PBEo-D3BJ24 and confirmed as energy minima by analytical harmonic vibrational frequency calculations settings: SCF=Tight, Int=UltraFine, (Gaussian og Opt=Tight). Within the geometry optimizations and frequency calculations, def2-TZVP basis sets²⁵ were applied except for the NPh2,NPh2'-BhPy+ system, where def2-SVP basis sets were used.²⁵ Because of convergence problems in the case of the optimization of Me-BnPy+ with Gaussian og, geometries and vibrational frequencies of the corresponding species were computed with ORCA 4.0 (ORCA 4.0 settings: VeryTightSCF, GRID7, TightOpt). If multiple conformers were conceivable for one compound, their relative stabilities were assessed on the basis of PBEo-D₃BJ calculations and only the most stable geometry was considered further. For the R,R'-BhPy+ ions investigated by TCID experiments (R,R' = H,H'; Me,Me'; H,OMe'), structures relevant to their dissociation reactions were re-optimized with B₃LYP²⁶ using 6-311+G(d,p) basis sets²⁷ and also confirmed as energy minima by the corresponding analytical harmonic vibrational frequency calculations.

For all PBEo-D₃BJ optimized structures, SPEs were calculated with the DLPNO-CCSD(T) method²⁸ (ORCA 4.0 settings: RHF, VeryTightSCF, TightPNO). These calculations were performed with cc-pVTZ as well as cc-pVQZ basis sets²⁹ in combination with the corresponding ccpVnZ/C auxiliary basis sets³⁰ (except for NPh2,NPh2'-BhPy+ system, where cc-pVDZ,29 cc-pVTZ and the corresponding cc-pVnZ/C basis sets³⁰ were employed). This procedure allowed us to determine DLPNO-CCSD(T) SPEs at the complete basis set (CBS) limit by using two-point extrapolations for the Hartree-Fock and the correlation energy as implemented in ORCA 4.0 (for details, see the Supporting Information).31 In the following, CBS(X,Y) denotes energies derived from the results of the calculations for cc-pVXZ and cc-pVYZ basis sets (X,Y = T,O or D,T). For each compound, the zero-point corrected energy, Ho, was calculated as the sum of the DLPNO-CCSD(T)/CBS(X,Y) SPE and the zero-point vibrational energy obtained from the PBEo-D₃BJ harmonic vibrational frequency calculation.

In addition, relaxed and partially unrelaxed potential energy surface scans for the pyridine loss of H,H'-BhPy+ and H-BnPy+ were conducted with the PBEo-D3BJ/def2-SVP method. Within these scans, the distance d(C-N) between the benzylic carbon atom and the pyridine nitrogen was increased in 0.1 Å steps up to +10 Å relative to the equilibrium bond length. For selected structures obtained from the scans, DLPNO-CCSD(T)/cc-pVTZ SPEs were calculated.

Synthesis of Thermometer Ions. Benzhydrylpyridinium ions were prepared by the treatment of R,R'-BhCl and NPh₂,NPh₂'-Bh⁺BF₄⁻ with pyridine (for details and analytical data, see the Supporting Information, Figures S₁-S₇). Apart from the commercially available H,H'-BhCl, the benzhydrylpyridinium precursors were provided by the Mayr group (LMU Munich). Benzylpyri-

dinium chlorides were synthesized according to methods outlined by Wysocki and coworkers.³² All other chemicals and solvents (HPLC grade) were used as purchased.

TCID Measurements. Experiments were carried out on two guided ion beam tandem mass spectrometers (GIBMS), described in detail previously, and referred to here as GIBMS133-36 and GIBMS2.35-37 Ions were generated with an ESI source, with differences between the respective ESI sources and the following ion-transfer regions^{38,39} of the two instruments explicitly discussed below. In both cases, acetonitrile solutions were infused by a syringepump at a flow rate of ~0.1 mL h-1 through a 35-gauge stainless steel needle, biased at a voltage of approximately 2 kV between the needle and instrument inlet. The inlet capillaries on both instruments were heated to ~350 K. Ions entered the first differentially-pumped stage (~10⁻² Torr) of the instruments through the capillary, and were subsequently collected and focused into radiofrequency (rf)-hexapoles using 88-plate rf ion funnels (IFs).^{38,40} The two instruments differ in the placement and length of the hexapoles: the GIBMS1 hexapole (14 cm in total length) spans two differentially-pumped regions (where the second is ~10⁻⁴ Torr),³⁸ whereas the two coupled hexapoles of GIBMS2 (~36 cm in total length) span only the first differentially-pumped region at ~10⁻² Torr.³⁹ The part of the hexapole that spans the high-pressure region of the GIBMS1 source is approximately one third the length of the two coupled hexapoles in GIBMS2. Thus, at the same pressure, the ions in GIBMS2 should undergo about a factor of three more collisions (on the order of 104) as those in GIBMS1. The unique feature of GIBMS1 is a hexapole that spans two differentially-pumped regions, such that ions are thermalized at ~300 K with narrow kinetic energy distributions. 17,38,41 In contrast, the temperature of the ions produced by GIBMS2 has not been characterized previously. In both instruments, ions were subsequently mass selected using a magnetic sector momentum analyzer. The GIBMS1 magnet can select precursor ions with up to only $m/z \sim 250$, whereas for GIBMS₂, this range extends to $m/z \sim 1000.37$ Because the m/z ratios of the Me,Me'-BhPy+ and H,OMe'-BhPy+ ions are higher than the GIBMS1 range, studies were also performed on GIBMS2 using the newly designed ESI/IF/hexapole source.³⁹ Prior to entering an rf-octopole ion beam guide, ions were decelerated to a controlled and well-defined kinetic energy. A reaction cell, in which Xe gas was introduced for the TCID experiments, partly surrounds the octopole. Measurements were typically performed in duplicate at Xe pressures of ~0.05, 0.1, and 0.2 mTorr, which are sufficiently low to ensure predominantly single collisions. Precursor and resulting product ions reaching the octopole exit were extracted and analyzed using a quadrupole mass analyzer. Ion intensities were measured with a Daly detector. 42 GIBMS133,34 and GIBMS237 differ in the length of the octopoles, with average ion flight times from the reaction cell to the quadrupole analyzer in each instrument estimated as 500 µs and 100 µs, respectively.36 Precursor and product ion intensities were measured as a function of precursor ion kinetic energy in the laboratory

(Lab) frame. As previously detailed,³³ these intensities were background corrected and converted to cross sections (with absolute and relative uncertainties estimated as 20% and 5%, respectively) as a function of energy in the center-of-mass (CM) frame. The data were processed and converted to cross sections in two ways: using the experimentally measured energy-dependent precursor ion intensity and assuming a constant precursor ion intensity, i.e., the average precursor intensity as determined for energies above the absolute zero in the energy scale. Reported modeling parameters (see below) were determined from the average of the values obtained from these two analyses. The full width at half maximum (FWHM) of the precursor ion kinetic energy distribution was measured using a retarding technique that has been described before,33 and also allows for the determination of the absolute zero in the energy scale (with a ±0.05 eV uncertainty in the lab frame). The FWHM values of the precursor ion kinetic energy distributions differed slightly for the two instruments with typical values of ~0.1-0.2 eV (Lab) and ~0.3-0.4 eV (Lab) obtained on GIBMS1 and GIBMS2, respectively. These differences are attributed primarily to where the ions are extracted from the hexapole (which essentially defines the zero of the kinetic energy scale of the reactant ions). In GIBMS1, because the ions are extracted in a low pressure region (~10⁻⁴ Torr), they undergo few collisions; whereas in GIBMS2, extraction occurs at ~10⁻² Torr, such that ions can undergo collisions in the extraction field, leading to a broader distribution of energies.

TCID Data Analysis. Threshold dissociation energies at o K, E_0 , were determined from fitting the energy dependent cross sections with a modified line-of-centers model that incorporates Rice-Ramsperger-Kassel-Marcus (RRKM) theory to account for kinetic shift effects. This modeling has been discussed in detail previously, 43-44 where eq. (2) is used to model the data:

$$\sigma(E) = \frac{n \sigma_0}{E} \sum_i g_i \int_{E_0 - E_i}^{E} P_d \cdot (E - \varepsilon)^{n-1} d(\varepsilon)$$
 (2)

Here, E corresponds to the relative kinetic energy of the reactants, σ_0 and n are scaling parameters, where the latter is related to the efficiency of the collisional energy transfer,³⁴ E_i corresponds to the rotational and vibrational energy of the reactants for state i with population fraction g_i such that $\Sigma g_i = 1$, ε is the energy converted from translational into internal energy, P_d is the dissociation probability given by $P_d = 1 - \exp[-k(E^*)\tau]$ where $E^* = E_i + \varepsilon$ is the internal energy of the energized molecule (EM), τ is the available experimental dissociation time (500 and 100 μ s for GIBMS1 and GIBMS2, respectively), and $k(E^*)$ is the unimolecular dissociation rate constant. The latter is obtained from RRKM theory using eq. (3):

$$k(E^*) = \frac{d N^{\dagger}(E^* - E_0)}{h \rho(E^*)}$$
 (3)

with d corresponding to the reaction degeneracy, $N^{\dagger}(E^* - E_o)$ is the sum of rovibrational states of the transition state (TS), and $\rho(E^*)$ is the density of states of the

EM. Similar to the previous TCID study on benzylpyridinium ions,17 vibrational frequencies (scaled by 0.989) and rotational constants needed for the modeling were obtained from the B₃LYP/6-311+G(d,p) calculations detailed above. Modeling was performed on zero-pressure extrapolated cross sections resulting in eight independent data sets. 45 CID of the benzhydrylpyridinium ions studied here results in cleavage of the C-N bond and exclusive loss of pyridine. As demonstrated by our quantum chemical calculations (see below), this dissociation proceeds via a loose TS, which is modeled at the phase space limit (PSL) and treated as product like with the transitional modes treated as rotors.7,4344 Within the PSL calculations, ion-dipole and ion-induced dipole interactions between the products were taken into account. For pyridine, a dipole moment of 2.190 D and a polarizability of 9.493 Å³ were used.⁴⁶ Moreover, the applied $k(E^*)$ values were obtained by integrating $k(E^*,J)$ over a statistical distribution of angular momenta J. E_0 , n, and σ_0 in eq. (2) were varied and optimized fits to the experimental cross sections were obtained using a non-linear least squares method. Uncertainties in the reported E_o values were determined from fits to independent data sets, from varying the n parameter by ± 0.1 , scaling the precursor ion vibrational frequencies by ±10%, scaling together the vibrational frequencies for the EM and TS by ±10%, scaling the ion time-of-flight up and down by a factor of 2, and by including the uncertainty in the energy scale (±0.05 eV, Lab).

Kinetic Shift Calculations. Microcanonical dissociation rate constants, k(E), for pyridine loss from R,R'-BhPy⁺ and R-BnPy+ were calculated as described above for the modeling of the TCID data. Either the computed E_o values and the geometries/vibrational frequencies obtained from the PBEo-D₃BJ calculations or the experimentally determined threshold energies and the B₃LYP/6-311+G(d,p) geometries/vibrational frequencies (scaled by 0.989) were used in these calculations. Appearance energies of dissociation, E_{app} , relevant to our survival yield measurements (see below) were calculated as energies for which $k(E_{\rm app}) = 1/\tau$ holds (the difference between $E_{\rm app}$ and $E_{\rm o}$ corresponds to the energy of the kinetic shift, $E_{\rm ks}$).^{5,8c} The experimental time window τ for ESI-induced dissociation processes in the commercial instrument (see below) was assumed to be 100 µs, similar to earlier thermometer-ion studies with an ESI quadrupole mass spectrometer.8c,e,h We conservatively estimate the uncertainty of the applied τ value to be a factor of 5 and therefore determined upper and lower limits of the appearance energies for $\tau = 20$ and 500 μs.

Survival Yield Measurements and Analysis. An equimolar mixture of benzhydryl- and benzylpyridinium compounds (individual concentrations of 1 mM) in dichloromethane or methanol, respectively, was treated with AgPF₆ (1.0 equiv. relative to the total concentration in Cl⁻) to effect the precipitation of AgCl and suppress the formation of unwanted $(R,R'-BhPy)_nCl_{n-1}^+$ (n = 2, 3) aggregates during the ESI process. The resulting supernatant solution was directly injected (flow rate of 0.3 mL h⁻¹) into

the ESI source of a micrOTOF-Q II mass spectrometer (Bruker Daltonics) located in Göttingen. Under standard conditions, the ESI source was operated (see the Supporting Information) with an ESI voltage of -4500 V and nitrogen acting both as nebulizer gas (500 Torr backing pressure) and dry gas (323 K, 5.0 L min⁻¹). Generated ions entered the instrument and passed two rf IFs, a quadrupole mass filter, and a quadrupole-ion guide containing a low pressure of nitrogen gas⁴⁷ before reaching a time-offlight (TOF) mass analyzer in a reflectron configuration. Positive-ion mode mass spectra were recorded over a mass range of m/z = 50-1500 for 1 min in quadruplicate and analyzed with the Compass Data Analysis 4.2 software package (Bruker Daltonics). For each measurement, the survival yields of the benzhydryl- and benzylpyridinium ions were determined according to eq. (1), with the reported error bars corresponding to one standard deviation. The mean survival yields of the thermometer ions were then plotted against their E_{app} values for $\tau = 20$, 100 and 500 µs, respectively, and fitted to a logistic regression function in each case (see the Supporting Information). From the derivatives of the logistic regressions obtained for the different experimental time scales, the mean and FWHM of the internal energy distribution of the thermometer ions (including the uncertainties of these values) as well as their approximate temperatures were determined (see the Supporting Information for details). In addition, the survival yields were also correlated with E_0 instead of E_{app} energies.

RESULTS AND DISCUSSION

Computed Threshold Energies. The potential energy surface scans for the pyridine loss from the benzhydrylpyridinium ion H,H'-BhPy $^+$ revealed that the C–N bond cleavage features no reverse barrier, which was also explicitly confirmed to be the case for H-BnPy $^+$ (Figure S8). Consequently, for this type of process, threshold energies, E_o , were calculated as reaction enthalpies ΔH^o and a loose TS model was applied for the calculations of microcanonical dissociation rate constants as detailed above. In addition, our quantum chemical calculations clearly indicate that the formation of a tropylium moiety in the course of the pyridine loss of H,H'-BhPy $^+$ ions can be already excluded for thermochemical reasons (Figure S9) and does not have to be considered further in the present context.

As we were aiming for thermometer ions with lower dissociation energies than those of the benzylpyridinium ions, we only considered benzhydrylpyridinium ions, R,R'-BhPy⁺, with electron-neutral or electron-donating substituents (R,R' = H,H'; Me,Me'; H,OMe'; Me,OMe'; OMe,OMe'; NPh₂,NPh₂'). A stronger electron-donating character of the substituents is expected to increase the stability of the R,R'-Bh⁺ fragment ions and, therefore, to lower the dissociation energy of the R,R'-BhPy⁺ precursor ions. Our computed E_0 values for the pyridine-loss reactions of these systems are in the range of 0.70–1.74 eV (Table 1, Table S1) and, thus, below the calculated E_0 range of 1.85–2.87 eV, which we obtained for a representa-

tive set of R-BnPy⁺ ions (R = NO₂, CN, H, Cl, Me, OMe; Table 1, Table S1). The good agreement of the calculated E_o values for the latter with the results from TCID experiments¹⁷ (Table 1) and former CCSD(T) studies^{14,16} points to the high accuracy⁴⁸ of the present DLPNO-CCSD(T)/CBS calculations.

Table 1. Computed threshold energies, E_0 , for the pyridine loss of benzhydryl- and benzylpyridinium ions. Experimental values for the latter are given for comparison.

R,R'-BhPy+	E _o (eV) calc ^a	R-BnPy ⁺	$E_{\rm o}$ (eV) calc ^a	$E_{\rm o}$ (eV) TCID b
H,H'	1.74	NO ₂	2.87	3.04 ± 0.12
Me,Me'	1.52	CN	2.78	
H,OMe'	1.41	Н	2.52	2.58 ± 0.15
Me,OMe'	1.33	Cl	2.41	
OMe,OMe'	1.18	Me	2.26	2.26 ± 0.13
NPh2,NPh2'	0.70	OMe	1.85	1.93 ± 0.08

^aResults from DLPNO-CCSD(T)/CBS//PBEo-D₃BJ calculations, for applied structures, see Figure S10. ^bExperimental values from ref. 17.

In line with expectations, the calculated relative gasphase stabilities of the benzhydrylpyridinium ions inversely correlate with the electrofugality parameters, $E_{\rm f}$, of the corresponding benzhydrylium ions. As Mayr and coworkers have shown, the $E_{\rm f}$ parameters themselves show a linear correlation with the sum of the Hammett constants $\Sigma \sigma^+$ for the substituents R,R' of each species. These relationships can be used to identify further R,R'-BhPy+ ions with higher or lower $E_{\rm o}$ values than those considered here.

Temperature Calibration of GIBMS2. TCID experiments were performed with two different GIBMS instruments, GIBMS1 and GIBMS2, equipped with ESI sources (see above). While GIBMS1 produces ions at a temperature of ~300 K after thermalization, 17,38,41 the temperature of the ions generated by GIBMS2 with its newly designed ESI source and thermalization region 39 has not been characterized yet. As H,H'-BhPy+ is sufficiently light to be investigated with both GIBMS instruments (see above), the thermochemistry measured for this thermometer ion on GIBMS1 can be used to calibrate the temperature of the ions produced by GIBMS2.

A representative composite of resulting zero-pressure extrapolated CID cross sections for H,H'-BhPy⁺ measured on GIBMS1 and GIBMS2 is shown in Figure 1. Here, within the energy range studied, CID of H,H'-BhPy⁺ results in exclusive loss of pyridine. As shown in Figure 1, the product ion cross sections for H,H'-BhPy⁺ measured on the two instruments have similar apparent thresholds and reach similar absolute magnitudes at high energies. Modeling the data from GIBMS1 with eq. (2) using a precursor ion temperature of 300 K yields an E_0 value of 1.79 ± 0.11 eV (Figure 1, black dashed line). In contrast, an E_0 value of 1.70 ± 0.10 eV is obtained when the data measured on GIBMS2 are modeled using a temperature of 300 K (Figure 1, red dashed line). This lower o K threshold

dissociation energy suggests that the temperature of the ions produced by GIBMS2 is underestimated in the modeling. Indeed, modeling these data with a precursor ion temperature of 360 K instead reproduces the $E_{\rm o}$ value from the GIBMS1 results, yielding an $E_{\rm o}$ value of 1.79 ± 0.10 eV (Figure 1, blue dashed line). The optimized modeling parameters of eq. (2) for H,H'-BhPy⁺ discussed here and for all other systems investigated are given in Table 2. From the molecular parameters of the reactant complexes and PSL TSs, we also derived entropies of activation, ΔS^{\dagger} , which are fully consistent with loose transition states.

The comparison for the H,H'-BhPy+ data suggests that the ions produced by GIBMS2 after thermalization are hotter by about ~60 K than those from the GIBMS1 source. As mentioned above, one of the differences between the two instruments is that the hexapole for GIBMS1 spans two vacuum regions.³⁸ In contrast, for GIBMS2 the two coupled hexapoles39 span only the highpressure region. Thus, the ions likely undergo collisional heating as they are transferred from the 10-2 Torr source region into the higher vacuum region of the GIBMS2 instrument, as also suggested by the larger FWHM (see above). This is also consistent with previous observations, where precursor ions with wider kinetic energy distributions were produced when the hexapole was located only in the 10⁻² Torr source region.³⁸ The H,H'-BhPy⁺ results allow the temperature of the ions produced by GIBMS2 to be calibrated. Thus, in subsequent analysis of additional systems studied with GIBMS2, the thermochemistry was determined by modeling the cross sections using a precursor ion temperature of 360 K.

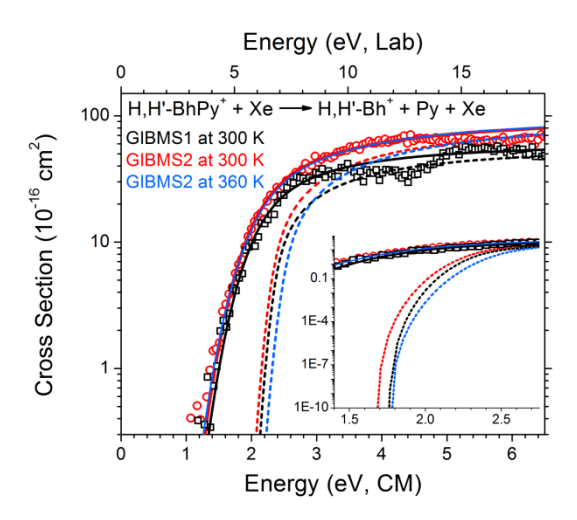


Figure 1. Representative zero-pressure extrapolated cross sections resulting from CID of H,H'-BhPy⁺ measured on two different instruments, GIBMS1 (black squares) and GIBMS2 (red circles), as a function of kinetic energy in the center-of-mass (CM, lower x-axis) and laboratory (Lab, upper x-axis) frames. Optimized fits to the experimental cross sections using eq. (2) are indicated by the solid (dashed) lines, which include (exclude) convolution over reactant internal and kinetic energies. The results from GIBMS2 are modeled using precursor ion temperatures of 300 (red lines) and 360 K (blue lines). Solid red and blue lines are superimposable. Inset is

an expansion to more clearly show the o K threshold dissociation energies from the models (dashed lines).

Table 2. Summary of optimized parameters from eq. (2) for models of TCID cross sections for the pyridine loss of benzhydrylpyridinium ions. Entropies of dissociation at 1000 K, ΔS^{\dagger} , are also given.

R,R'- BhPy ⁺	Instr. (T in K)	E _o (eV)	$\sigma_{ m o}{}^a$	n	$\Delta S^{\dagger \ b}$
H,H'	MS1 (300)	1.79 ± 0.11	88 ± 19	0.9 ± 0.1	81 ± 4
	MS2 (300)	1.70 ± 0.10	113 ± 13	0.9 ± 0.1	81 ± 4
	MS2 (360)	1.79 ± 0.10	117 ± 14	0.9 ± 0.1	81 ± 4
Me,Me'	MS2 (360)	1.55 ± 0.13	154 ± 30	1.0 ± 0.2	78 ± 4
H,OMe'	MS2 (360)	1.37 ± 0.14	145 ± 30	0.9 ± 0.2	82 ± 4

 $^a\sigma_{\rm o}$ in 10⁻¹⁶ cm². $^b\Delta S^\dagger$ in J mol⁻¹ K⁻¹.

Experimental Threshold Energies. TCID experiments were performed additionally on Me,Me'-BhPy+ and H,OMe'-BhPy⁺ using GIBMS2. Within the energy range studied, CID of these ions also results in exclusive loss of pyridine. The resulting zero-pressure extrapolated cross sections as a function of energy in the CM frame for all three benzhydrylpyridinium ions (R,R' = H,H'; Me,Me'; H,OMe') are shown in Figure 2. There is a shift to lower energies in the apparent thresholds with different para substitution of these ions following the order H,H' > Me,Me' > H,OMe'. At elevated energies, the CID cross sections of all three ions approach a similar maximum magnitude, as would be expected on the basis of their similar sizes. Modeling the data using the calibrated ion temperature of 360 K for the GIBMS2 source (Figure 2), gives E_0 values of 1.55 \pm 0.13 eV and 1.37 \pm 0.14 eV (Table 1) for Me,Me'-BhPy+ and H,OMe'-BhPy+, respectively. Here, the uncertainties include the propagated uncertainty in the source temperature from the calibration using the GIBMS1 results (for details, see the Supporting Information).

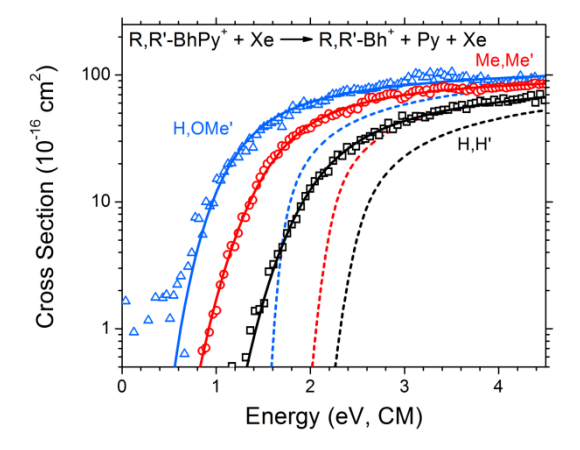


Figure 2. A composite of zero-pressure extrapolated cross sections (measured with GIBMS2) resulting from CID of R,R'-BhPy⁺ where R,R' = H,H' (black squares), Me,Me' (red circles), and H,OMe' (blue triangles) as a function of kinetic energy in the center-of-mass (CM) frame. Optimized fits to the experimental cross sections using eq. (2) are indicated by the solid (dashed) lines, which include (exclude) convolution

over reactant internal and kinetic energies. Cross sections are modeled using a precursor ion temperature of 360 K.

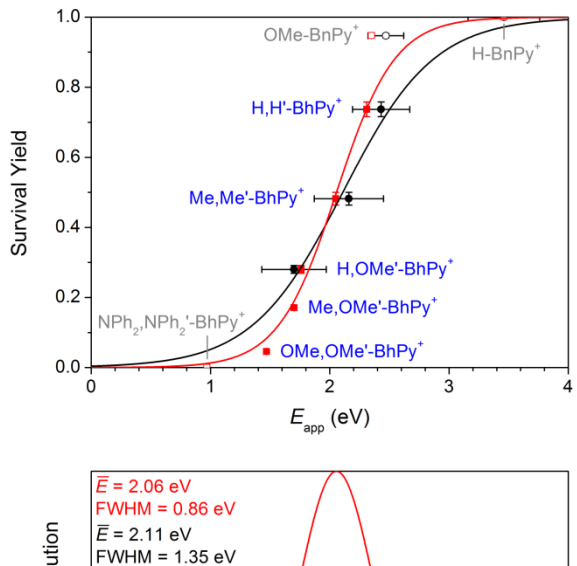
Computational vs. Experimental Results. The calculated E_0 values for the pyridine loss of the experimentally investigated R,R'-BhPy⁺ ions (R,R' = H,H'; Me,Me'; H,OMe'; Table 1) are all within the experimental uncertainty of the results from the TCID study (Table 2). In total, a mean absolute deviation of only 0.04 eV has been obtained for the computed threshold energies with respect to the experimental values, which feature a mean uncertainty of 0.13 eV (the result from GIBMS1 is considered for R,R' = H,H'). This excellent agreement between experiment and theory shows that our DLPNO-CCSD(T)/CBS//PBEo-D₃BJ calculations yield accurate threshold energies for the dissociation of benzhydrylpyridinium ions. Therefore, the computed E_0 values for the R,R'-BhPy⁺ ions that were not studied experimentally $(R,R' = Me,OMe'; OMe,OMe'; NPh_2,NPh_2'; Table 1)$, are also considered reliable. This conclusion matches the expected accuracy of our computational approach for reaction energies of closed-shell organic molecules.⁴⁸

Computed Kinetic Shifts. For the estimated experimental time window $\tau = 100 \, \mu s$, the rate calculations on the basis of the calculated threshold energies yielded kinetic shift energies, E_{ks} , for the pyridine loss of benzhydrylpyridinium ions in the range of 0.27-0.57 eV (Figure S11, top, Table S2). As it is usually the case for such loose TS dissociations, higher E_o values and more internal degrees of freedom of the precursor ions increase the kinetic shift. As very similar threshold energies were obtained both from theory and experiments, the two sets lead to comparable E_{ks} values (Figure 12, Table S2). For the pyridine loss from the considered benzylpyridinium ions, the kinetic shift energies derived from the calculated $E_{\rm o}$ values were predicted to be in the range of 0.50–1.57 eV for $\tau = 100 \,\mu s$ (Figure S11, bottom, Table S2), similar to those found in the previous TCID study.¹⁷ In contrast, earlier studies had arrived at much higher E_{ks} values for these latter reactions when considering a similar experimental time scale as here, even though they assumed incorrectly small threshold energies.8c,e For example, kinetic shift energies of 1.04 and 1.38 eV were predicted for the pyridine loss of OMe-BnPy+on the basis of E_o values of 1.30 and 1.55 eV, respectively, 8c,e whereas we calculated $E_{\rm ks}$ = 0.50 eV ($E_{\rm o}$ = 1.85 eV) for this system. The reason for the overestimation of calculated kinetic shifts in earlier studies^{8c,e,g,h} is the application of a wrong TS model, namely, a variant of rigid-activated complex RRKM theory, which is not appropriate for describing reactions with no reverse barrier, such as the loss of pyridine from R-BnPy+and R,R'-BhPy+ ions. Instead, such reactions should be modeled with the assumption of a loose TS at the phase space limit. Indeed, this approach results in TCID threshold energies of R,R'-BhPy+ and R-BnPy+ ions, that are in agreement with the E_0 values from reliable quantum chemical calculations, as demonstrated in the present and previous work.17

Internal Energy of Ions Produced with a Commercial ESI Mass Spectrometer. For determining the inter-

nal energies of the new thermometer ions after ESI and transfer to the mass analyzer of a commercial hybrid quadrupole-TOF instrument (see above), we probed solutions in dichloromethane and methanol. The latter is a solvent typically applied for ESI, while the former has been extensively used for studying the stability of R,R'-Bh⁺ ions and their adducts.20 To be useful for the characterization of the ESI process, the R,R'-BhPy⁺ thermometer ions need to be stable in solution. ¹H NMR measurements confirmed that R,R'-BhPy⁺ ions (R,R' = H,H'; Me,Me'; H,OMe'; Me,OMe'; OMe,OMe') remain intact in dichloromethane at mM concentrations (Figure S7). The stability of these systems in dichloromethane and in methanol was also evident from the solutions being colorless; the R,R'-Bh+ fragment ions are intensely colored.20b In contrast, the NMR-spectroscopic experiments on NPh₂,NPh₂'-BhPy⁺ pointed to the presence of significant amounts of its benzhydrylium fragment ion in dichloromethane. This result is fully in line with the known dissociation constant of NPh2, NPh2'-BhPy+ in this solvent.214 Despite this complication, a survival yield of o could be assigned to this system (see below) because the ESI mass spectra did not show any NPh2,NPh2'-BhPy+ ions.

The ESI mass spectra recorded for solutions of the R,R'-BhPy+ and R-BnPy+ ions under standard conditions permitted the determination of survival yields in a straightforward manner. The survival yields for the benzhydryl- and benzylpyridinium ions displayed unimodal distributions in the range between o and 1 (Figure 3, top, and Figures S13-S17; see Figures S18 and S19 for representative raw data). Plotting the survival yields against the $E_{\rm app}$ values derived from the computed $E_{\rm o}$ energies (Tables S2-S4) furnished the expected sigmoidal curves, which could be fitted well by logistic functions (Figure 3, top, red squares and line, and Figures S13-S17). For the actual fitting, we only included the R,R'-BhPy+ data (R,R' = H,H'; Me,Me'; H,OMe'; Me,OMe'; OMe,OMe') to avoid possible problems arising from different numbers of degrees of freedom (DOF) of the thermometer ions. If the DOF numbers differ too much, significantly different energy distributions would result for the individual thermometer ions under thermal conditions and, thus, could impair the analysis.⁵ From the fits, we can derive internal energy distributions of the ions characterized by mean values of $2.06 \pm 0.13/1.88 \pm 0.11 \text{ eV}$ and FWHMs of $o.86 \pm o.07/o.86 \pm o.06$ eV for dichloromethane/methanol (Figure 3, bottom, red line, and Figure S13-S17). These energy distributions can be compared to Maxwell-Boltzmann distributions for temperatures between $620 \pm 20/590 \pm 20$ and $710 \pm 20/680 \pm 20$ K (Figures S20-S23).⁴⁹ The similar behavior found for dichloromethane and methanol suggests that solvent effects play only a minor role. The lower internal energies and temperatures determined for methanol possibly indicate an enhanced evaporative cooling for this solvent, in accordance with its higher evaporation enthalpy.⁵⁰ Preliminary studies show that variations of the ESI and ion-transfer conditions have only minor effects (changes of the mean energy of no more than ±0.10 eV for methanol as the solvent).⁵¹



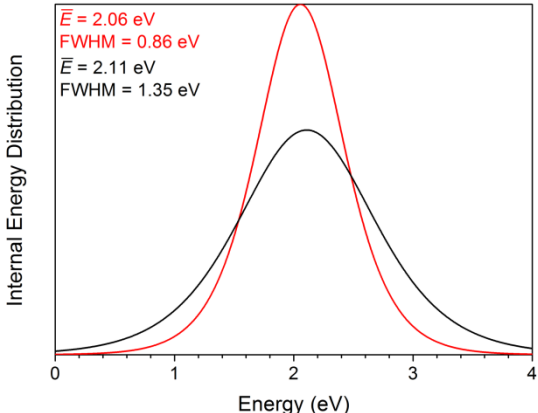


Figure 3. Top: Measured survival yields for the applied thermometer ions (sprayed from dichloromethane) plotted against the appearance energies (for $\tau = 100~\mu s$) obtained on the basis of calculated (red squares) and experimental E_0 values (black circles), and logistic regressions (red and black line; $R^2 = 0.98$ and 0.91, respectively). For the regression analysis, only the data points represented by filled symbols were considered. Bottom: Derived internal energy distributions (red and black line).

If the survival yield analysis is based on E_{app} values derived from the experimentally determined (instead of the computed) E₀ values (Table S2–S4), internal energy distributions with similar mean values $2.11 \pm 0.19/1.84 \pm 0.16 \text{ eV}$ (dichloromethane/methanol) are obtained (Figure 3, top, black squares and line, and Figure S13-S17). However, the lack of data points at low E_{app} values imposes less restrictions on the fits and, thus, leads to significantly broadened **FWHMs** of $1.35 \pm 0.11/1.42 \pm 0.12 \text{ eV}.$

Plots of the survival yields against the two sets of threshold energies $E_{\rm o}$ (computed and experimental, Tables 1 and 2, respectively) could also be modeled by logistic functions and afforded energy distributions, which were shifted to lower energies by approx. 0.5 eV relative to those derived from correlations with the appearance energies $E_{\rm app}$ (Figures S24 and S25). Thus, the neglect of kinetic shifts changes the determined internal energies to a relatively moderate extent.

CONCLUSION

Benzhydrylpyridinium ions R,R'-BhPy+ are proposed as new thermometer ions for the characterization of the ESI process. Quantum chemical calculations at the DLPNO-CCSD(T)/CBS//PBEo-D₃BJ level confirmed that their dissociation energies (loss of pyridine) are significantly lower than those of the corresponding benzylpyridinium ions R'-BnPy+. Further calculations indicated that the dissociation reactions proceed via loose transition states and that the kinetic shifts associated with the fragmentation of the R,R'-BhPv⁺ ions are only moderate for typical experimental time windows. TCID measurements for selected systems afforded threshold energies in quantitative agreement with the theoretical results and, thus, corroborate the latter. The measurements performed with two different GIB mass spectrometers could also be used to characterize the temperature of ions produced in the ESI/IF/hexapole source of one of the two instruments for the first time.

A set of five different benzhydrylpyridinium ions were then employed to determine the internal energies of ions generated in the ESI source of a commercial quadrupole-TOF hybrid mass spectrometer. A survival-yield analysis based upon the computed $E_{\rm app}$ energies found energy distributions with maxima at 2.06 ± 0.13/1.88 ± 0.11 eV and FWHMs of 0.86 ± 0.07/0.86 ± 0.06 eV (dichloromethane/methanol) for an operation under standard conditions. The use of benzhydrylpyridinium ions as thermometer ions holds great promise for the characterization of the ESI process using different configurations and further mild ionization methods.

ASSOCIATED CONTENT

Supporting Information

The Supporting Information is available free of charge on the ACS Publication website at DOI: 10.1021/acs.anal-chemXXXXXXX.

Complete basis set limit extrapolation, synthesis and analytical data of benzhydrylpyridinium salts, ¹H NMR studies of benzhydrylpyridinium compounds, details of survival yield measurements and analysis, further results from quantum chemical calculations, propagation of uncertainty in ion temperature for GIBMS2 thermochemistry, further results from kinetic shift calculations, further results from survival yield measurements and analysis (PDF)

XYZ coordinates (in Å) and harmonic vibrational frequencies (in cm⁻¹) of the calculated structures (ZIP)

AUTHOR INFORMATION

Corresponding Authors

*E-mail: armentrout@chem.utah.edu

*E-mail: konrad.koszinowski@chemie.uni-goettingen.de

ORCID

P. B. Armentrout: 0000-0003-2953-6039 K. Koszinowski: 0000-0001-7352-5789

Author Contributions

§R.R., T.A. and M.D. contributed equally.

Notes

The authors declare no competing financial interest.

ACKNOWLEDGMENT

The authors acknowledge support for this work by the National Science Foundation, Grant CHE-1664618 (PBA) and by the DFG, 389479699/GRK2455 (TA, KK). We thank the Mayr Group (LMU Munich) for the generous donation of benzhydrylpyridinium precursors, Dr. Friedrich Kreyenschmidt for the synthesis of benzylpyridinium chlorides and Prof. Dr. Ricardo Mata for carrying out a few of the DLPNO-CCSD(T) calculations. Dedicated to Professor Richard N. Zare on the occasion of his 80th birthday.

REFERENCES

- (1) (a) Yamashita, M.; Fenn, J. B. *J. Phys. Chem.* **1984**, *88*, 4451-4459. (b) Yamashita, M.; Fenn, J. B. *J. Phys. Chem.* **1984**, *88*, 4671-4675. (c) Fenn, J. B. *Angew. Chem.*, *Int. Ed.* **2003**, *42*, 3871-3894.
- (2) Kebarle, P.; Verkerk, U. H. Mass Spectrom. Rev. 2009, 28, 898-917.
- (3) (a) Wang, R.; Zenobi, R. *J. Am. Soc. Mass Spectrom.* **2010**, 21, 378-385 (b) Gibson, S. C.; Feigerle, C. S.; Cook, K. D. *Anal. Chem.* **2014**, 86, 464-472. (c) Soleilhac, A.; Dagany, X.; Dugourd, P.; Girod, M.; Antoine, R. *Anal. Chem.* **2015**, 87, 8210-8217.
- (4) (a) Kenttämaa, H. I.; Cooks R. G. Int. J. Mass Spectrom Ion Processes 1985, 64, 79-83. (b) Wysocki, V. H.; Kenttämaa, H. I.; Cooks R. G. Int. J. Mass Spectrom. Ion Processes 1987, 75, 181-208. (c) Cooks, R. G.; Ast T.; Kralj, B.; Kramer, V.; Žigon, D. J. Am. Soc. Mass Spectrom. 1990, 1, 16-27.
- (5) Gabelica, V.; De Pauw, E. Mass Spectrom. Rev. 2005, 24, 566-587.
 - (6) Lifshitz, C. Mass Spectrom. Rev. 1982, 1, 309-348
- (7) Rodgers, M. T.; Ervin, K. M.; Armentrout, P. B. *J. Chem. Phys.* **1997**, *106*, 4499-4508.
- (8) (a) Derwa, F.; De Pauw, E.; Natalis, P. Org. Mass Spectrom. 1991, 26, 117-118. (b) Collette, C.; De Pauw; E. Rapid Commun. Mass Spectrom. 1998, 12, 165-170. (c) Collette, C.; Drahos, L.; De Pauw, E.; Vékey, K. Rapid Commun. Mass Spectrom. 1998, 12, 1673-1678. (d) Gabelica, V.; De Pauw, E.; Karas, M.; Int. J. Mass Spectrom. 2004, 231, 189-195. (e) Naban-Maillet, J.; Lesage, D.; Bossée, A.; Gimbert, Y.; Sztáray, J.; Vékey, K.; Tabet, J.-C. J. Mass Spectrom. 2005, 40, 1-8. (f) Touboul, D.; Jecklin, M. C.; Zenobi, R. Rapid Commun. Mass Spectrom. 2008, 22, 1062-1068. (g) Rondeau, D.; Galland, N.; Zins, E.-L.; Pepe, C.; Drahos, L.; Vékey, K. J. Mass. Spectrom. 2011, 46, 100-111. (h) Rondeau, D.; Drahos, L.; Vékey, K. Rapid Commun. Mass Spectrom. 2014, 28, 1273-1284.
- (9) (a) Barylyuk, K. V.; Chingin, K.; Balabin, R. M.; Zenobi, R. *J. Am. Soc. Mass Spectrom.* **2010**, *21*, 172-177. (b) Zins, E.-L.; Pepe, C.; Schröder, D. *J. Mass. Spectrom.* **2010**, *45*, 1253-1260.
- (10) The occurrence of rearrangement reactions affording thermochemically favored tropylium ions before the dissociation of benzylpyridinium ions has been excluded: Morsa, D.; Gabelica, V.; Rosu, F.; Oomens, J.; De Pauw, E. *J. Phys. Chem. Lett.* **2014**, 5, 3787-3791.
- (11) Luo, G.; Marginean, I.; Vertes, A. Anal. Chem. 2002, 74, 6185-6190.
- (12) Nefliu, M.; Smith, J. N.; Venter, A.; Cooks, R. G. *J. Am. Soc. Mass Spectrom.* **2008**, *19*, 420-427.
- (13) Harris, G. A.; Hostetler, D. M.; Hampton, C. Y.; Fernández, F. M. *J Am. Soc. Mass Spectrom.* **2010**, *21*, 855-863.
- (14) Huang, Y.; Yoon, S. H.; Heron, S. R.; Masselon, C. D.; Edgar, J. S.; Tureček, F.; Goodlett, D. R. *J. Am. Soc. Mass Spectrom.* **2012**, 23,1062-1070.

- (15) Katritzky, A. R.; Watson, C. H.; Dega-Szafran, Z.; Eyler, J. R. J. Am. Chem. Soc. 1990, 112, 2471-2478.
- (16) DeBord, J. D.; Verkhoturov, S. V.; Perez, L. M.; North, S. W.; Hall, M. B.; Schweikert, E. A. J. Chem. Phys. 2013, 138, 214301.
- (17) Carpenter, J. E.; McNary, C. P.; Furin, A.; Sweeney, A. F.; Armentrout, P. B. J. Am. Soc. Mass Spectrom. **2017**, 28, 1876-1888.
- (18) An alternative strategy to access thermometer ions with weakened C–N bonds relies on the substitution of pyridine by less nucleophilic amines, such as NH₃. Stephens et al. realized this concept by introducing R-BnNH₃⁺ as new thermometer ions, for which they calculated dissociation energies in the range of $1.1 \le E_0 \le 2.0.19$ These thermometer ions can be produced by the protonation of neutral R-BnNH₂ precursors, which is advantageous for their use for the characterization of plasma-based ionization methods. In contrast, the propensity of thermometer ions to undergo proton transfer reactions would prove detrimental if applied to the characterization of the energetic conditions of the ESI process.
- (19) Stephens, E. R.; Dumlao, M.; Xiao, D.; Zhang, D.; Donald, W. A. J. Am. Soc. Mass Spectrom. 2015, 26, 2081-2084.
- (20) (a) Mayr, H.; Patz, M. Angew. Chem., Int. Ed. Engl.1994, 33, 938-957. (b) Mayr, H.; Bug, T.; Gotta, M. F.; Hering, N.; Irrgang, B.; Janker, B.; Kempf, B.; Loos, R.; Ofial, A. R.; Remennikov, G.; Schimmel, H. J. Am. Chem. Soc. 2001, 123, 9500-9512. (c) Streidl, N.; Denegri, B.; Kronja, O.; Mayr, H. Acc. Chem. Res. 2010, 43, 1537-1549. (d) Ammer, J.; Nolte, C.; Mayr, H. J. Am. Chem. Soc. 2012, 134, 13902-1391. (e) Mayr, H. Tetrahedron 2015, 71, 5095-511. (f) Mayr, H.; Ofial, A. R. Acc. Chem. Res. 2016, 49, 952-965.
- (21) (a) Brotzel, F.; Kempf, B.; Singer, T.; Zipse, H.; Mayr, H. *Chem. Eur. J.* **2007**, *1*3, 336-345. (b) Follet, E.; Zipse, H.; Lakhdar, S.; Ofial, A. R.; Berionni, G. *Synthesis* **2017**, *49*, 3495-3504.
- (22) Gaussian 09, revision D.01; Gaussian Inc: Wallingford, CT, 2013.
- (23) (a) Neese, F. Wiley Interdiscip. Rev.: Comput. Mol. Sci. 2012, 2, 73-78. (b) Neese, F. Wiley Interdiscip. Rev.: Comput. Mol. Sci. 2018. DOI: 10.1002/wcms.1327. (c) ORCA, version 4.0; Max Planck Institute for Chemical Energy Conversion: Mülheim a. d. Ruhr, Germany, 2017.
- (24) (a) Adamo, C.; Barone, V. *J. Chem. Phys.* **1999**, *110*, 6158-6170. (b) Grimme, S.; Antony, J.; Ehrlich, S.; Krieg, H. *J. Chem. Phys.* **2010**, *132*, 154104. (c) Grimme, S.; Ehrlich, S.; Goerigk, L. *J. Comput. Chem.* **2011**, *32*, 1456-1465.
- (25) Weigend, F.; Ahlrichs, R. Phys. Chem. Chem. Phys. 2005, 7, 3297-3305.
- (26) (a) Becke, A. D. *J. Chem. Phys.* **1993**, *98*, 5648-5652. (b) Stephens, P. J.; Devlin, F. J.; Chabalowski, C. F.; Frisch, M. J. *J. Phys. Chem.* **1994**, *98*, 11623-11627.
- (27) (a) Krishnan, R.; Binkley, J. S.; Seeger, R.; Pople, J. A. *J. Chem. Phys.* **1980**, 72, 650-654. (b) Clark, T.; Chandrasekhar, J.; Spitznagel, G. W.; Schleyer, P. v. R. *J. Comput. Chem.* **1983**, 4, 294-301. (c) Frisch, M. J.; Pople, J. A.; Binkley, J. S. *J. Chem. Phys.* **1984**, 80, 3265-3269.
- (28) (a) Riplinger, C.; Neese, F. *J. Chem. Phys.* **2013**, *138*, 034106. (b) Riplinger, C.; Sandhoefer, B.; Hansen, A.; Neese, F. *J. Chem. Phys.* **2013**, *139*, 134101. (c) Riplinger, C.; Pinski, P.; Becker, U.; Valeev, E. F.; Neese, F. *J. Chem. Phys.* **2016**, *144*, 024109.
- (29) (a) Dunning, T. H., Jr. *J. Chem. Phys.* **1989**, *90*, 1007-1023. (b) Woon, D. E.; Dunning, T. H., Jr. *J. Chem. Phys.* **1993**, *98*, 1358-1371.
- (30) Weigend, F.; Köhn, A.; Hättig, C. *J. Chem. Phys.* **2002**, *116*, 3175-3183.
- (31) Neese, F.; Valeev, E. F. *J. Chem. Theory Comput.* **2011**, *7*, 33-43.
- (32) Dagan, S.; Hua, Y.; Boday, D. J.; Somogyi, A.; Wysocki, R. J.; Wysocki, V. H. *Int. J. Mass Spectrom.* 2009, 283, 200-205.

- (33) Ervin, K. M.; Armentrout, P. B. J. Chem. Phys. 1985, 83, 166-189.
- (34) Muntean, F.; Armentrout, P. B. J. Chem. Phys. 2001, 115, 1213-1228.
- (35) Armentrout, P. B. Int. J. Mass Spectrom. 2000, 200, 219-241.
- (36) Armentrout, P. B. J. Am. Soc. Mass Spectrom. 2002, 13, 419-434.
- (37) Loh, S. K.; Hales, D. A.; Lian, L.; Armentrout, P. B. *J. Chem. Phys.* **1989**, *90*, 5466-5485.
- (38) Moision, R. M.; Armentrout, P. B. *J. Am. Soc. Mass Spectrom.* **2007**, *18*, 1124-1134.
- (39) McNary, C. P. Ph.D. Dissertation, University of Utah, 2017.
- (40) Shaffer, S. A.; Prior, D. C.; Anderson, G. A.; Udseth, H. R.; Smith, R. D. *Anal. Chem.* **1998**, 70, 4111-4119.
- (41) Ye, S. J.; Armentrout, P. B. *J. Phys. Chem. A* **2008**, *112*, 3587-3596.
 - (42) Daly, N. R. Rev. Sci. Instrum. 1960, 31, 264-267.
- (43) Rodgers, M. T.; Ervin, K. M.; Armentrout, P. B. J. Chem. *Phys.* **1997**, *106*, 4499-4508.
- (44) Rodgers, M. T.; Armentrout, P. B. *J. Chem. Phys.* **1998**, 109, 1787-1800.
- (45) Hales, D. A.; Lian, L.; Armentrout, P. B. *Int. J. Mass Spectrom. Ion Processes* **1990**, *102*, 269-301.
- (46) NIST Computational Chemistry Comparison and Benchmark Database, NIST Standard Reference Database Number 101 Release 19. http://cccbdb.nist.gov/ (accessed November 9, 2018).
- (47) The nitrogen gas is needed to achieve high signal intensities by confining the ions to central trajectories. If an extra voltage is applied to the quadrupole-ion guide, it can be also used as a collision cell, but no such voltage was applied in present experiments.
- (48) (a) Liakos, D. G.; Sparta, M.; Kesharwani, M. K.; Martin, J. M. L.; Neese, F. *J. Chem. Theory Comput.* **2015**, 11, 1525-1539. (b) Paulechka, E.; Kazakov, A. *J. Phys. Chem. A.* **2017**, 121, 4379-4387. (c) Minenkov, Y.; Wang, H.; Wang, Z.; Sarathy, S. M.; Cavallo, L. *J. Chem. Theory Comput.* **2017**, 13, 3537-3560.
- (49) The given error bars are derived from the analysis of the Me,Me'-BhPy+ results and supposed to be representative for all cases
- (50) CRC Handbook of Chemistry and Physics; Haynes, W. M., Ed.; CRC Press: Boca Raton, 2012.
- (51) Specifically, we varied the flow rate of the dry gas, the ESI capillary voltage, the amplitudes of the RF voltages applied to the components of the ion-transfer optics, and the time of the ion transfer into the TOF analyzer over the range $x_i(\min)$ to $x_i(\max)$, with typically $x_i(\max)/x_i(\min) \ge 2$.